

Article

Genome-Wide Identification and Expression Analysis of the Broad-Complex, Tramtrack, and Bric-à-Brac Domain-Containing Protein Gene Family in Potato

Aiana ¹, Anita Katwal ¹, Hanny Chauhan ¹ , Santosh Kumar Upadhyay ²  and Kashmir Singh ^{1,*} 

¹ Department of Biotechnology, BMS Block I, Panjab University, Sector 25, Chandigarh 160014, India; aianagill53@gmail.com (A.); katwalsabu99@gmail.com (A.K.); hannysingh31@gmail.com (H.C.)

² Department of Botany, Panjab University, Sector 14, Chandigarh 160014, India; skupadhyay@pu.ac.in

* Correspondence: kashmirbio@pu.ac.in or kashmir123@gmail.com; Tel.: +91-172-2534085 or +91-950-1684096

Abstract: The BTB (broad-complex, tramtrack, and bric-à-brac) domain, also known as the POZ (POX virus and zinc finger) domain, is a conserved protein–protein interaction domain present in various organisms. In this study, we conducted a genome-wide search to identify and characterize *BTB* genes in *Solanum tuberosum*. A total of 57 *StBTBs* were identified and analyzed for their physicochemical properties, chromosomal distribution, gene structure, conserved motifs, phylogenetic relationships, tissue-specific expression patterns, and responses to hormonal and stress treatments. We found that *StBTBs* were unevenly distributed across potato chromosomes and exhibited diverse gene structures and conserved motifs. Tissue-specific expression analysis revealed differential expression patterns across various potato tissues, implying their roles in plant growth and development. Furthermore, differential expression analysis under hormonal and stress treatments indicated the involvement of *StBTBs* in abiotic and biotic stress responses and hormone signaling pathways. Protein–protein interaction analysis identified potential interactions with ribosomal proteins, suggesting roles in translational regulation. Additionally, microRNA target site analysis revealed regulatory relationships between *StBTBs* and miRNAs. Our study provides a comprehensive understanding of the *StBTB* gene family in potato, laying the groundwork for further functional characterization and manipulation of these genes to improve stress tolerance and agricultural productivity in potato and related plant species.

Keywords: *Solanum tuberosum*; BTB domain; abiotic stress; biotic stress; protein modification



Citation: Aiana, Katwal, A.; Chauhan, H.; Upadhyay, S.K.; Singh, K. Genome-Wide Identification and Expression Analysis of the Broad-Complex, Tramtrack, and Bric-à-Brac Domain-Containing Protein Gene Family in Potato. *Agriculture* **2024**, *14*, 771. <https://doi.org/10.3390/agriculture14050771>

Academic Editors: Xiaoyong Xu, Lijuan Jiang and Lun Wang

Received: 5 April 2024
Revised: 13 May 2024
Accepted: 15 May 2024
Published: 16 May 2024



Copyright: © 2024 by the authors. Licensee MDPI, Basel, Switzerland. This article is an open access article distributed under the terms and conditions of the Creative Commons Attribution (CC BY) license (<https://creativecommons.org/licenses/by/4.0/>).

1. Introduction

The BTB domain (broad-complex, tramtrack, and bric-à-brac) is a conserved domain which was first identified in the *Drosophila* broad-complex, tramtrack, and bric-à-brac genes [1,2]. A total of 183 BTB proteins were found in *Homo sapiens*, 195 in *Mus musculus*, 178 in *Caenorhabditis elegans*, 77 in *Arabidopsis thaliana*, and 5 in *Saccharomyces cerevisiae* [3]. The structure of the BTB domain consists of five conserved alpha helices and three beta strands along with extension regions at N- and C-terminal sites. The BTB domain consists of 116 amino acids and acts as a homodimer or heterodimer to interact with various other non-BTB proteins to perform various functions [4]. The BTB domain serves two functions: it has the capability to self-assemble into a dimer and to engage with proteins lacking the BTB domain. Given that the conserved groove within the BTB domain resides at the interface of the dimer, it has been anticipated that the formation of dimers is crucial for the envisaged interactions occurring within this groove [5]. BTB domains undergo particular adaptations, acquiring novel functions such as the multimerization of proteins engaged in DNA binding and ion channel activity [6].

The BTB domain is recognized for its capacity to facilitate protein–protein interactions. Within plants, BTB domain-containing proteins engage with a range of partner

proteins, such as transcription factors, kinases, and other regulatory molecules. These interactions frequently take place via the BTB domain, facilitating the assembly of multi-protein complexes crucial for diverse cellular functions. BTB domain-containing proteins frequently serve as substrate adaptors for Cullin-RING E3 ubiquitin ligases (CRLs) within the ubiquitin–proteasome system (UPS). Through the BTB domain, they selectively recruit target proteins to the CRL complex, triggering their ubiquitination and subsequent breakdown by the 26S proteasome [7]. This process tightly controls the levels of pivotal regulatory proteins crucial for governing plant growth, development, and responses to stress. Certain BTB domain-containing proteins function as transcriptional regulators by modulating the function of transcription factors. They have the capacity to act as either co-repressors or co-activators, thereby impacting the expression of target genes involved in diverse physiological processes. By interacting with transcription factors or chromatin-modifying enzymes, BTB domain-containing proteins govern gene expression through modulation of chromatin structure or transcriptional activity [8].

BTB is a protein–protein interaction domain as it interacts with other domains like NPH3 (non-phototropic hypocotyl 3), BACK (for BTB and C-terminal Kelch), TAZ (Transcription Adaptor putative zinc finger), MATH (meprin and TRAF homology), SKP1 (S-phase kinase-associated protein 1), and ARM (armadillo) to perform important roles in plant growth and development [9]. Previous studies have shown that plants overexpressing the *BT2* (BTB AND TAZ DOMAIN PROTEIN 2) gene have reduced nitrogen uptake efficiency under limiting nitrate conditions as compared to wild type plants [10]. The BTB domain plays an important role in transcriptional regulation [11], chromatin remodeling, cytoskeleton regulation [3], lymphocyte development [12], axon guidance [13], leukemia [14], and protein ubiquitination [15]. The BTB domain is essential for gametophytic development in plants [14,16] and provides abiotic and biotic stress tolerance [17–21]. Various BTB domain-containing proteins help regulate plant signaling mediated by hormones such as abscisic acid, jasmonic acid, gibberellic acid, and salicylic acid [17].

Plants suffer from various types of biotic and abiotic stresses, which result in both qualitative and quantitative losses of crops. Abiotic stresses like drought stress and heat stress cause huge damage to the potato crop and reduce its yield. *IbBT4*, a BTB-TAZ domain protein-encoding gene from sweet potato, was shown to provide drought tolerance in transgenic Arabidopsis [18]. *AtSIBP1* is a novel BTB domain-containing gene whose overexpression significantly elevated the expression of stress-responsive genes, indicating its role as a positive regulator in salt stress responses [19]. Previous studies show that overexpression of BTB domain-containing protein NPR1 in Arabidopsis leads to resistance against *Pseudomonas syringae*, *Peronospora parasitica*, and *Erysiphe cichoracearum* [20]. The overexpression of *NbBTB* in *Nicotiana benthamiana* resulted in enhanced susceptibility to *P. parasitica* infection, whereas the silencing of *NbBTB* led to higher resistance to *P. parasitica*, suggesting that *NbBTB* plays a suppressive role in the plant's innate defence mechanisms [21]. It was also observed that *NbBTB* was specifically implicated in the basal defence response against oomycete infections as either its overexpression or silencing did not have any impact on plant resistance against the bacterial pathogens *Ralstonia solanacearum* and *P. syringae*. The hypersensitive reaction (HR) elicited by avirulence proteins from *R. solanacearum* and *Phytophthora infestans* was shown to be decreased by the expression of *NbBTB*. Conversely, the silencing of *NbBTB* resulted in the opposite effect, suggesting its negative regulatory role in effector-triggered immunity (ETI). The protein accumulation of avirulence effectors in plants with silenced *NbBTB* was found to be dramatically increased, indicating that it is likely to exert a detrimental influence on effector protein accumulation and, consequently, the effector-triggered immunity (ETI) response [21].

This study aims at performing a genome-wide search to identify *BTBs* in potato and analyzing their chromosomal distribution, gene structure, conserved motif analysis, phylogenetic analysis, protein–protein interactions, and miRNA target prediction. Furthermore, the expression patterns of the identified genes were studied under specific plant tissues,

hormonal treatments, and various abiotic and biotic stress treatments. The present investigation presents a comprehensive analysis of the *BTB* gene family, offering a robust foundation for the systematic investigation and functional characterization of *BTBs* in potato and other related plant species.

2. Materials and Methods

2.1. Identification and Sequence Analysis of the *StBTB* Gene Family

The *Solanum tuberosum* genome (DM v6.1) was downloaded from the Spud database (http://spuddb.uga.edu/dm_v6_1_download.shtml, accessed on 9 September 2023). *BTBs* were identified by conducting a standalone HMMER [22] search against the protein database of potato using the Pfam ID PF00651. The putative *StBTB* protein sequences were checked for the presence of a conserved BTB domain using the NCBI protein Batch CD-Search database (<https://www.ncbi.nlm.nih.gov/Structure/bwrpsb/bwrpsb.cgi>, accessed on 10 October 2023) [23], InterProScan (<https://www.ebi.ac.uk/interpro/>, accessed on 10 October 2023) [24], and SMART (<http://smart.embl-heidelberg.de/>, accessed on 10 October 2023) [25]. The protein sequences of the resulting genes were used to analyze the physicochemical properties using the ExPASy ProtParam tool (<https://web.expasy.org/protparam/>, accessed on 15 October 2023) [26]. The subcellular location of all BTB proteins was investigated using WolfPSORT (<https://www.genscript.com/wolf-psort.html>, accessed on 12 October 2023) [27]. SOPMA was used to understand the secondary structure composition of *StBTB* proteins (https://npsa-prabi.ibcp.fr/cgi-bin/npsa_automat.pl?page=/NPSA/npsa_sopma.html, accessed on 14 October 2023) [28].

2.2. Chromosomal Distribution and Gene Duplication Event

The chromosomal locations of all identified *StBTBs* were retrieved from the Spud database (http://spuddb.uga.edu/dm_v6_1_download.shtml, accessed on 12 October 2023). Bidirectional BLAST was performed using the identified *StBTBs* and the genes showing >80% similarity were considered to be duplicated. Duplicated genes situated within a 5 megabase (Mb) range on the same chromosome were classified as tandem duplications, whereas those found beyond the 5 Mb threshold were categorized as segmental duplications [29]. The positions of all the genes along with duplications were mapped on their respective chromosomes using TBTools-II v2.010 software [30]. The ratio of the number of nonsynonymous substitutions per nonsynonymous site (K_a) to the number of synonymous substitutions per synonymous site (K_s) of the duplicated gene pairs was calculated using TBTools-II v2.010 software [30].

2.3. Gene Structure and Conserved Motif Analyses of the *StBTBs*

The genomic and coding sequences of the identified *StBTBs* were retrieved from the Spud database and were used to study the intron–exon organization using GSDS 2.0 (<http://gsds.gao-lab.org/>, accessed on 16 October 2023) [31]. The *StBTB* protein sequences were used to analyze the conserved motifs using MEME Suite (version 5.4.1) (<https://meme-suite.org/meme/index.html>, accessed on 17 October 2023) with default parameters except the number of motifs was set to 20 and the width of the motifs was set from 20 to 200 [32]. The resulting motifs were visualized using TBTools-II v2.010 software [30].

2.4. Multiple Sequence Alignment and Phylogenetic Tree Construction

Multiple sequence alignment of the *StBTB* protein sequences was performed using the MUSCLE algorithm [33]. A neighbor-joining phylogenetic tree was constructed with the Mega-X v2.1 software using the p-distance method with pairwise deletion and 1000 bootstrap replications [34]. The phylogenetic tree was visualized using i-TOL (<https://itol.embl.de/>, accessed on 9 January 2024) [35].

2.5. Tissue-Specific Expression Analysis of *StBTBs*

The tissue-specific gene expression values (TPM) for RNA-seq libraries of potato DM v6.1 were retrieved from the Spud database (http://spuddb.uga.edu/dm_v6_1_download.shtml, accessed on 9 January 2024) for 16 different tissues (stamen, flower, mature tuber, tuber sprout, young tuber, tuber pith, leaf, water-stressed leaf, tuber peel, shoot apex, stem, stolon, petiole, tuber cortex, root, whole in vitro plant) from the plant. The retrieved TPMs of *StBTBs* were then plotted as heatmaps on a log scale using TBTools-II v2.010 software [30].

2.6. Expression Analysis of *StBTBs* under Various Hormonal and Stress Treatments

The gene expression values (TPM) for RNA-seq libraries of potato DM v6.1 were retrieved from the Spud database (http://spuddb.uga.edu/dm_v6_1_download.shtml, accessed on 9 January 2024) for various hormonal treatments, i.e., IAA, GA3, BAP, and ABA. The gene expression values of potato under heat stress, salt stress, and mannitol treatment were also retrieved. Additionally, the TPMs for *Phytophthora infestans* infected plants and systemic acquired resistance (SAR) elicitors such as BABA- and BTH-treated plants were also taken. All the retrieved *StBTB* TPMs were then plotted as heatmaps on a log scale using TBTools-II v2.010 software [30].

2.7. Protein–Protein Interaction and GO Analysis

The protein sequences of *StBTBs* were used to create a protein–protein network using the String database v12.0 (<https://string-db.org/>, accessed on 1 February 2024) with a high confidence score (0.700) and no more than 20 interactors [36]. The network was visualized using Cytoscape v3.9.1 software [37]. Pathway analysis and gene ontology analysis of all *StBTBs* under all three categories, namely “biological process”, “cellular component”, and “molecular function” were carried out using the OmicsBox2.2.4 software package (<https://www.biobam.com/omicsbox>, accessed on 31 October 2024).

2.8. microRNA Target Site Analysis

The coding sequences of *StBTBs* were searched against the published miRNAs in the pSRNATarget server (<https://www.zhaolab.org/psRNATarget/analysis>, accessed on 1 February 2024) to predict the miRNAs targeted by *StBTBs* [38]. The interactions were visualized using Cytoscape v3.9.1 software [37].

3. Results

3.1. Identification of *BTB* Genes in Potato and Their Sequence Analysis

An HMM search using PF00651 resulted in 57 putative *StBTBs* encoding 103 *BTB* proteins. The proteins with the highest number of amino acid residues were selected for each *BTB* gene for further analyses. The presence of *BTB* domains in the protein sequences of these 57 genes was further confirmed using the NCBI-CDD, SMART, and InterProScan databases. These genes were named from *StBTB1* to *StBTB57* based on their location on the potato chromosomes. The CDS length of *StBTBs* varied from 441 bp in *StBTB30* to 2598 bp in *StBTB2*, while the amino acid residues varied from 146 in *StBTB30* to 865 in *StBTB2* (Table 1). The molecular weight of proteins varied from 16.648 kDa in *StBTB30* to 94.892 kDa in *StBTB2*. The theoretical isoelectric point of the proteins ranged from 4.62 in *StBTB30* to 9.32 in *StBTB13*, while the instability index varied from 21.89 in *StBTB22* to 62.06 in *StBTB26*. *StBTB5* was found to have the lowest aliphatic index (74.09), while *StBTB29* had the highest aliphatic index (113.48). The highest GRAVY (grand average of hydropathicity) value was observed in *StBTB29*, which had a positive value of 0.125, while the lowest value was found in *StBTB9*, which had a negative value of 0.564 (Table S1). The subcellular localization analysis revealed that *StBTB* proteins were majorly found in the nucleus followed by the cytoplasm and chloroplast (Table 1). The secondary structure of most of the *StBTB* proteins mainly comprised of alpha helices (51.36%) followed by 35.53% random coils, 9.65% extended strands, and 3.46% beta turns (Table S2).

Table 1. Chromosomal location, CDS length, AA residues, and subcellular localization of *BTB* genes in potato.

Gene Name	SpudDB Accession Number	Chromosomal Location	CDS Length	AA Length	Subcellular Localization
<i>StBTB1</i>	Soltu.DM.01G005950.1 http://spuddb.uga.edu/cgi-bin/annotation_report.cgi?orf=Soltu.DM.01G005950.1 , (accessed on 12 October 2023)	1:6212257–6219717	1218	405	Cytoplasm
<i>StBTB2</i>	Soltu.DM.01G023290.1 http://spuddb.uga.edu/cgi-bin/annotation_report.cgi?orf=Soltu.DM.01G023290.1 , (accessed on 12 October 2023)	1:62115639–62125961	2598	865	Nucleus
<i>StBTB3</i>	Soltu.DM.01G023810.1 http://spuddb.uga.edu/cgi-bin/annotation_report.cgi?orf=Soltu.DM.01G023290.1 , (accessed on 12 October 2023)	1:62789505–62798820	1224	407	Chloroplast
<i>StBTB4</i>	Soltu.DM.01G029170.1 http://spuddb.uga.edu/cgi-bin/annotation_report.cgi?orf=Soltu.DM.01G029170.1 , (accessed on 12 October 2023)	1:68879361–68877284	1725	574	Chloroplast
<i>StBTB5</i>	Soltu.DM.01G034510.1 http://spuddb.uga.edu/cgi-bin/annotation_report.cgi?orf=Soltu.DM.01G034510.1 , (accessed on 12 October 2023)	1:74078735–74083692	1659	552	Nucleus
<i>StBTB6</i>	Soltu.DM.01G038390.1 http://spuddb.uga.edu/cgi-bin/annotation_report.cgi?orf=Soltu.DM.01G038390.1 , (accessed on 12 October 2023)	1:77301342–77303414	1665	554	Nucleus
<i>StBTB7</i>	Soltu.DM.01G046570.1 http://spuddb.uga.edu/cgi-bin/annotation_report.cgi?orf=Soltu.DM.01G046570.1 , (accessed on 12 October 2023)	1:84079985–84086687	1881	626	Nucleus
<i>StBTB8</i>	Soltu.DM.02G002620.1 http://spuddb.uga.edu/cgi-bin/annotation_report.cgi?orf=Soltu (accessed on 12 October 2023)	2:11879293–11874980	1890	629	Nucleus
<i>StBTB9</i>	Soltu.DM.02G003900.1 http://spuddb.uga.edu/cgi-bin/annotation_report.cgi?orf=Soltu.DM.02G003900.1 , (accessed on 12 October 2023)	2:15605796–15599933	840	279	Peroxisome
<i>StBTB10</i>	Soltu.DM.02G007630.1 http://spuddb.uga.edu/cgi-bin/annotation_report.cgi?orf=Soltu.DM.02G007630.1 , (accessed on 12 October 2023)	2:21886913–21882888	1275	424	Cytoplasm

Table 1. Cont.

Gene Name	SpudDB Accession Number	Chromosomal Location	CDS Length	AA Length	Subcellular Localization
<i>StBTB11</i>	Soltu.DM.02G012330.1 http://spuddb.uga.edu/cgi-bin/annotation_report.cgi?orf=Soltu.DM.02G012330.1 , (accessed on 12 October 2023)	2:27057682–27063283	1746	581	Nucleus
<i>StBTB12</i>	Soltu.DM.02G027710.1 http://spuddb.uga.edu/cgi-bin/annotation_report.cgi?orf=Soltu.DM.02G027710.1 , (accessed on 12 October 2023)	2:40452119–40448666	1467	488	Chloroplast
<i>StBTB13</i>	Soltu.DM.02G027750.1 http://spuddb.uga.edu/cgi-bin/annotation_report.cgi?orf=Soltu.DM.02G027750.1 , (accessed on 12 October 2023)	2:40471945–40474925	1137	378	Nucleus
<i>StBTB14</i>	Soltu.DM.02G027770.1 http://spuddb.uga.edu/cgi-bin/annotation_report.cgi?orf=Soltu.DM.02G027770.1 , (accessed on 12 October 2023)	2:40517486–40522346	1842	613	Chloroplast
<i>StBTB15</i>	Soltu.DM.02G027830.1 http://spuddb.uga.edu/cgi-bin/annotation_report.cgi?orf=Soltu.DM.02G027830.1 , (accessed on 12 October 2023)	2:40600737–40596954	1791	596	Nucleus
<i>StBTB16</i>	Soltu.DM.02G027880.1 http://spuddb.uga.edu/cgi-bin/annotation_report.cgi?orf=Soltu.DM.02G027880.1 , (accessed on 12 October 2023)	2:40646109–40645050	501	166	Nucleus
<i>StBTB17</i>	Soltu.DM.03G005510.1 http://spuddb.uga.edu/cgi-bin/annotation_report.cgi?orf=Soltu.DM.03G005510.1 , (accessed on 12 October 2023)	3:6670844–6676484	1884	627	Cytoplasm
<i>StBTB18</i>	Soltu.DM.03G025100.1 http://spuddb.uga.edu/cgi-bin/annotation_report.cgi?orf=Soltu.DM.03G025100.1 , (accessed on 12 October 2023)	3:50328857–50331675	1038	345	Nucleus
<i>StBTB19</i>	Soltu.DM.04G012100.1 http://spuddb.uga.edu/cgi-bin/annotation_report.cgi?orf=Soltu.DM.04G012100.1 , (accessed on 12 October 2023)	4:13482468–13485467	1386	461	Cytoplasm
<i>StBTB20</i>	Soltu.DM.04G037630.1 http://spuddb.uga.edu/cgi-bin/annotation_report.cgi?orf=Soltu.DM.04G037630.1 , (accessed on 12 October 2023)	4:68525044–68518203	2415	804	Chloroplast

Table 1. Cont.

Gene Name	SpudDB Accession Number	Chromosomal Location	CDS Length	AA Length	Subcellular Localization
<i>StBTB21</i>	Soltu.DM.05G021440.1 http://spuddb.uga.edu/cgi-bin/annotation_report.cgi?orf=Soltu.DM.05G021440.1 , (accessed on 12 October 2023)	5:49859963–49865413	1446	481	Nucleus
<i>StBTB22</i>	Soltu.DM.05G022360.1 http://spuddb.uga.edu/cgi-bin/annotation_report.cgi?orf=Soltu.DM.05G022360.1 , (accessed on 12 October 2023)	5:50791378–50794505	801	266	Cytoplasm
<i>StBTB23</i>	Soltu.DM.05G022990.1 http://spuddb.uga.edu/cgi-bin/annotation_report.cgi?orf=Soltu.DM.05G022990.1 , (accessed on 12 October 2023)	5:51463053–51457832	1023	340	Nucleus
<i>StBTB24</i>	Soltu.DM.06G002220.1 http://spuddb.uga.edu/cgi-bin/annotation_report.cgi?orf=Soltu.DM.06G002220.1 , (accessed on 12 October 2023)	6:2651681–2655195	1800	599	Chloroplast
<i>StBTB25</i>	Soltu.DM.06G010640.1 http://spuddb.uga.edu/cgi-bin/annotation_report.cgi?orf=Soltu.DM.06G010640.1 , (accessed on 12 October 2023)	6:32043750–32040570	840	279	Chloroplast
<i>StBTB26</i>	Soltu.DM.06G026950.1 http://spuddb.uga.edu/cgi-bin/annotation_report.cgi?orf=Soltu.DM.06G026950.1 , (accessed on 12 October 2023)	6:52716023–52712688	1050	349	Nucleus
<i>StBTB27</i>	Soltu.DM.06G026960.1 http://spuddb.uga.edu/cgi-bin/annotation_report.cgi?orf=Soltu.DM.06G026960.1 , (accessed on 12 October 2023)	6:52723186–52718338	1050	349	Nucleus
<i>StBTB28</i>	Soltu.DM.06G028810.1 http://spuddb.uga.edu/cgi-bin/annotation_report.cgi?orf=Soltu.DM.06G028810.1 , (accessed on 12 October 2023)	6:54046853–54048811	1722	573	Chloroplast
<i>StBTB29</i>	Soltu.DM.06G034720.1 http://spuddb.uga.edu/cgi-bin/annotation_report.cgi?orf=Soltu.DM.06G034720.1 , (accessed on 12 October 2023)	6:58701505–58709231	1617	538	Chloroplast
<i>StBTB30</i>	Soltu.DM.06G034740.1 http://spuddb.uga.edu/cgi-bin/annotation_report.cgi?orf=Soltu.DM.06G034740.1 , (accessed on 12 October 2023)	6:58720995–58723523	441	146	Chloroplast

Table 1. Cont.

Gene Name	SpudDB Accession Number	Chromosomal Location	CDS Length	AA Length	Subcellular Localization
<i>StBTB31</i>	Soltu.DM.07G011890.1 http://spuddb.uga.edu/cgi-bin/annotation_report.cgi?orf=Soltu.DM.07G011890.1 , (accessed on 12 October 2023)	7:38290258–38273905	1884	627	Chloroplast
<i>StBTB32</i>	Soltu.DM.07G013880.1 http://spuddb.uga.edu/cgi-bin/annotation_report.cgi?orf=Soltu.DM.07G013880.1 , (accessed on 12 October 2023)	7:42990889–42988509	1731	576	Plastid
<i>StBTB33</i>	Soltu.DM.07G014680.1 http://spuddb.uga.edu/cgi-bin/annotation_report.cgi?orf=Soltu.DM.07G014680.1 , (accessed on 12 October 2023)	7:44408833–44404274	1728	575	Cytoplasm/Nucleus
<i>StBTB34</i>	Soltu.DM.07G016030.1 http://spuddb.uga.edu/cgi-bin/annotation_report.cgi?orf=Soltu.DM.07G016030.1 , (accessed on 12 October 2023)	7:46031384–46034171	2064	687	Chloroplast
<i>StBTB35</i>	Soltu.DM.07G016870.1 http://spuddb.uga.edu/cgi-bin/annotation_report.cgi?orf=Soltu.DM.07G016870.1 , (accessed on 12 October 2023)	7:46995457–47002655	1734	577	Cytoplasm
<i>StBTB36</i>	Soltu.DM.07G027790.1 http://spuddb.uga.edu/cgi-bin/annotation_report.cgi?orf=Soltu.DM.07G027790.1 , (accessed on 12 October 2023)	7:56826287–56828986	987	328	Cytoplasm
<i>StBTB37</i>	Soltu.DM.08G001470.1 http://spuddb.uga.edu/cgi-bin/annotation_report.cgi?orf=Soltu.DM.08G001470.1 , (accessed on 12 October 2023)	8:1948150–1941686	1848	615	Cytoplasm
<i>StBTB38</i>	Soltu.DM.08G006060.1 http://spuddb.uga.edu/cgi-bin/annotation_report.cgi?orf=Soltu.DM.08G006060.1 , (accessed on 12 October 2023)	8:8434101–8428805	1212	403	Cytoplasm
<i>StBTB39</i>	Soltu.DM.08G028580.1 http://spuddb.uga.edu/cgi-bin/annotation_report.cgi?orf=Soltu.DM.08G028580.1 , (accessed on 12 October 2023)	8:57912747–57917717	1560	519	Nucleus
<i>StBTB40</i>	Soltu.DM.08G028600.1 http://spuddb.uga.edu/cgi-bin/annotation_report.cgi?orf=Soltu.DM.08G028600.1 , (accessed on 12 October 2023)	8:57927168–57928872	1380	459	Chloroplast

Table 1. Cont.

Gene Name	SpudDB Accession Number	Chromosomal Location	CDS Length	AA Length	Subcellular Localization
<i>StBTB41</i>	Soltu.DM.08G028610.1 http://spuddb.uga.edu/cgi-bin/annotation_report.cgi?orf=Soltu.DM.08G028610.1 , (accessed on 12 October 2023)	8:57933232–57934873	1332	443	Chloroplast
<i>StBTB42</i>	Soltu.DM.09G005820.1 http://spuddb.uga.edu/cgi-bin/annotation_report.cgi?orf=Soltu.DM.09G005820.1 (accessed on 12 October 2023)	9:5410787–5407618	1785	594	Cytoplasm
<i>StBTB43</i>	Soltu.DM.09G011290.1 http://spuddb.uga.edu/cgi-bin/annotation_report.cgi?orf=Soltu.DM.09G011290.1 , (accessed on 12 October 2023)	9:19305560–19308657	1737	578	Vacuole
<i>StBTB44</i>	Soltu.DM.09G017950.1 http://spuddb.uga.edu/cgi-bin/annotation_report.cgi?orf=Soltu.DM.09G017950.1 , (accessed on 12 October 2023)	9:50663650–50660954	1824	607	Nucleus
<i>StBTB45</i>	Soltu.DM.09G019780.1 http://spuddb.uga.edu/cgi-bin/annotation_report.cgi?orf=Soltu.DM.09G019780.1 , (accessed on 12 October 2023)	9:54297721–54289424	2127	708	Cytoplasm
<i>StBTB46</i>	Soltu.DM.09G022320.1 http://spuddb.uga.edu/cgi-bin/annotation_report.cgi?orf=Soltu.DM.09G022320.1 , (accessed on 12 October 2023)	9:57831226–57825083	1236	411	Nucleus
<i>StBTB47</i>	Soltu.DM.09G023040.1 http://spuddb.uga.edu/cgi-bin/annotation_report.cgi?orf=Soltu.DM.09G023040.1 , (accessed on 12 October 2023)	9:58865131–58869419	1890	629	Chloroplast
<i>StBTB48</i>	Soltu.DM.10G000680.1 http://spuddb.uga.edu/cgi-bin/annotation_report.cgi?orf=Soltu.DM.10G000680.1 , (accessed on 12 October 2023)	10:619135–609397	2250	749	Plastid
<i>StBTB49</i>	Soltu.DM.10G005800.1 http://spuddb.uga.edu/cgi-bin/annotation_report.cgi?orf=Soltu.DM.10G005800.1 , (accessed on 12 October 2023)	10:5842039–5836297	1656	551	Nucleus
<i>StBTB50</i>	Soltu.DM.10G013480.1 http://spuddb.uga.edu/cgi-bin/annotation_report.cgi?orf=Soltu.DM.10G013480.1 , (accessed on 12 October 2023)	10:38866471–38857805	2349	782	Cytoplasm

Table 1. Cont.

Gene Name	SpudDB Accession Number	Chromosomal Location	CDS Length	AA Length	Subcellular Localization
<i>StBTB51</i>	Soltu.DM.10G021040.1 http://spuddb.uga.edu/cgi-bin/annotation_report.cgi?orf=Soltu.DM.10G021040.1 , (accessed on 12 October 2023)	10:52920912–52916854	1833	610	Nucleus
<i>StBTB52</i>	Soltu.DM.10G027630.1 http://spuddb.uga.edu/cgi-bin/annotation_report.cgi?orf=Soltu.DM.10G027630.1 , (accessed on 12 October 2023)	10:58822974–58825292	1464	487	Cytoplasm
<i>StBTB53</i>	Soltu.DM.10G027950.1 http://spuddb.uga.edu/cgi-bin/annotation_report.cgi?orf=Soltu.DM.10G027950.1 , (accessed on 12 October 2023)	10:59080668–59078099	1473	490	Nucleus
<i>StBTB54</i>	Soltu.DM.11G011280.1 http://spuddb.uga.edu/cgi-bin/annotation_report.cgi?orf=Soltu.DM.11G011280.1 , (accessed on 12 October 2023)	11:11798335–11794985	987	328	Cytoplasm
<i>StBTB55</i>	Soltu.DM.11G025060.1 http://spuddb.uga.edu/cgi-bin/annotation_report.cgi?orf=Soltu.DM.11G025060.1 , (accessed on 12 October 2023)	11:45125219–45116416	1227	408	Nucleus
<i>StBTB56</i>	Soltu.DM.12G008220.1 http://spuddb.uga.edu/cgi-bin/annotation_report.cgi?orf=Soltu.DM.12G008220.1 , (accessed on 12 October 2023)	12:7252303–7257056	1668	555	Nucleus
<i>StBTB57</i>	Soltu.DM.12G019670.1 http://spuddb.uga.edu/cgi-bin/annotation_report.cgi?orf=Soltu.DM.12G019670.1 , (accessed on 12 October 2023)	12:46941436–46943083	795	264	Cytoplasm

3.2. Chromosomal Mapping and Gene Duplication Analysis

The chromosomal locations and sequences of all *StBTBs* were retrieved from the Spud database (Table 1) and were mapped on their respective chromosomes (Figure 1). All the *StBTBs* were observed to be located unevenly on all 12 potato chromosomes. The maximum number of *StBTBs* (seven genes) were found on chromosome 2, followed by six genes on chromosomes 1 and 6. Chromosomes 7, 9, and 10 contained six genes, while chromosome 8 contained five *StBTBs*, followed by chromosome 8 with three genes. Chromosomes 3, 4, 11, and 12 contained the least number of *StBTBs* with two genes each. We observed nine duplicated *StBTB* gene pairs in potato. Out of the nine gene pairs, *StBTB15-StBTB16* and *StBTB40-StBTB41* were found to be tandemly duplicated, while the other seven gene pairs (*StBTB4-StBTB28*, *StBTB43-StBTB24*, *StBTB29-StBTB45*, *StBTB5-StBTB49*, *StBTB53-StBTB19*, *StBTB19-StBTB52*, and *StBTB1-StBTB55*) were found to be segmental duplications (Figure 1). All the duplicated gene pairs had a Ka/Ks ratio of less than one, indicating purifying selection. *StBTB43* and *StBTB24* showed a high sequence divergence value as their pS (synonymous variation within species) value is greater than 0.75.

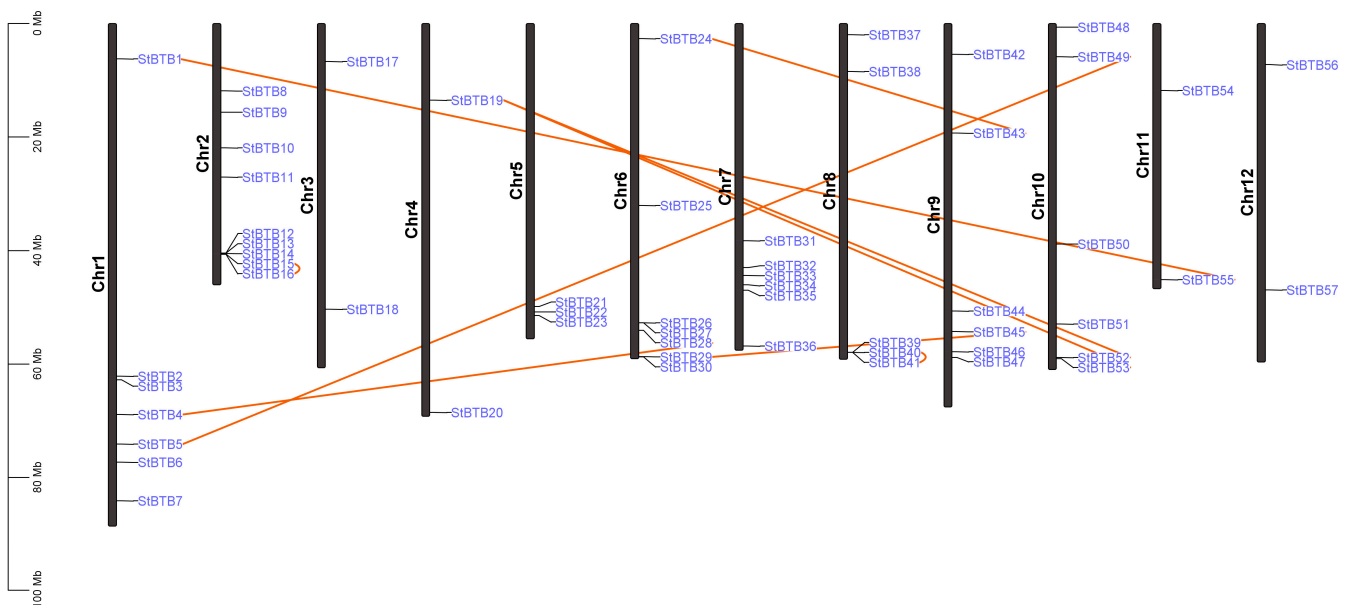


Figure 1. Distribution of *BTB* genes on potato chromosomes. Chromosome numbers are shown at the left of each bar with *StBTBs* on the right side represented in blue color. The vertical scale represents the size of chromosomes in megabases (Mb). The brown lines represent duplicated *StBTBs*.

3.3. Gene Structure and Conserved Motif Analysis

Intron–exon structure analysis was performed to study the gene structure of *StBTBs*. Significant variation was observed within *StBTBs* in terms of both intron length and intron numbers. *StBTB48* had the highest number of 18 introns, while four genes (*StBTB9*, *StBTB19*, *StBTB52*, and *StBTB53*) contained only one intron (Figure 2). In total, 42.1% of *StBTBs* were found to have three introns. *StBTB31* was constituted of the longest intron made up of 8771 bp.

Conserved motif analysis was performed using the sequences of all *StBTB* proteins (Figure 3). Motif 4 (BTB/POZ) was observed to be conserved throughout all the *StBTBs* except *StBTB21*, *StBTB30*, and *StBTB39*. Motifs 1, 2, 7, 8, 9, 18, and 20 (NPH3) were found to be distributed across 22 *StBTB* proteins, while motifs 3, 5, and 12 (POB1-like) were conserved across 30 *StBTB* proteins, motifs 13 and 14 (TAZ) were conserved across five *StBTB* proteins, motifs 15 and 16 (NPR5/6) were found to be conserved among six *StBTB* proteins, motif 6 (MATH/TRAF) was conserved within five *StBTB* proteins, motifs 10 and 17 (ARM) were seen to be present in 22 *StBTB* proteins, and motif 11 (AtSIBP1-like) was found in 26 *StBTB* proteins (Table 2).



Figure 2. Intron–exon structural organization of all *StBTBs*.

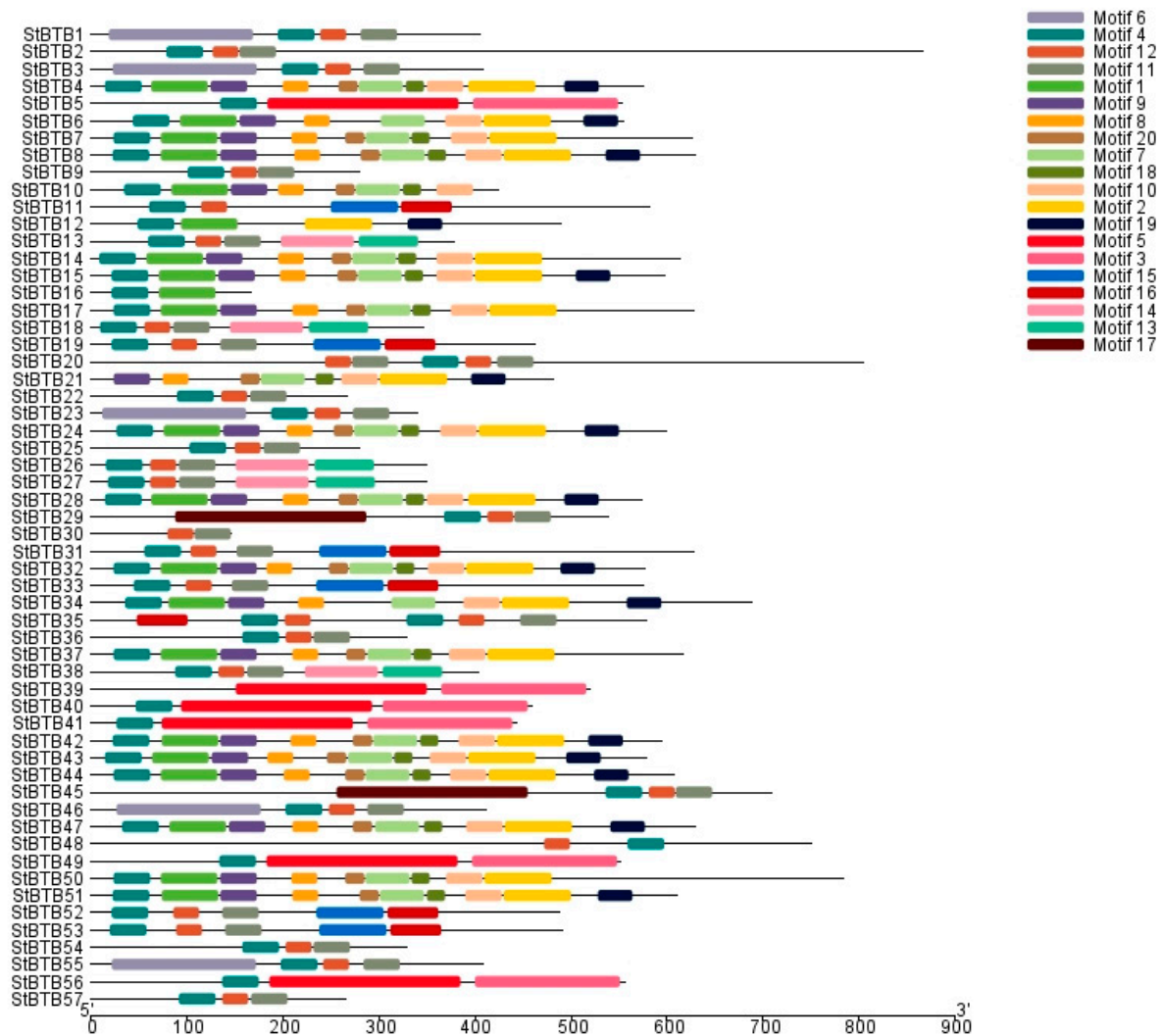


Figure 3. Distribution of 20 different motifs conserved across StBTB proteins.

Table 2. Sequence of conserved motifs present across StBTB proteins.

Motif No.	Motif Name	Sequence of Motifs
Motif 1	NPH3	IPGGAEAFELAAKFCYGVNFEJTAYNVAALRCAA EYLEMTEEYSKGNLISKTEVFLNSVV
Motif 2	NPH3	VPDYARPVHDGLYRAIDIY LKAHPGLSDSERKRLCKLMD CQKLSQEACTHAAQNERLPLRVIV QVLFFEQL
Motif 3	N.A.	YVERAYKYRPVKVLEFELPHQQCVVYLDLKRDECANLFPAGR VYSQAFHLGGQGFFLSAHCN MDQQSAFHCFGLFLGMQEKGSVSAVDYEFVAVRTKPGEEYVSKYKGN YFTFTGGKAVGYRNLFG IPWTPFLAEDSLYFINGILHLRAELTI
Motif 4	BTB	SELASDVTINVGGRSFHLHKFILAARSGVFRKLF SNGNE
Motif 5	BACK	IHASEEAALMDLLKFMYSNTLSTKTPPGLLDVLM AADKFEVASC MRYCSRELQNLPM TSESA LLYLDLPSSVLMADAVRPLADAAKQFLAARFKDITK FQEEVLSLPLAGIEAVLSSDDLQIASED AVYDFVLKWARHTHPKJEERREILTSRLCRLIRFPFMT CRKLRKVLTCNDFDHELASKFVLEAL FYKAEAPHRQ
Motif 6	MATH	TSSRSVTETVNGSHRFVINGYSLAKGMGIGKYITSDTFTVGGHQWAIYFYPDGKNPEDNSTYVS LFIALASEGTDVRALFELTLIDQSGKGKHKVHSHFDRALES GPYTLKYR GSMWGYKRFFRRALLE TSDYLKDDCLKIHCTVGVVRS T
Motif 7	NPH3	SVPCSFLKLLRS AIMLDAS PSCRSE LERRIGLQLDQATLBDLLIPA
Motif 8	NPH3	DWWVEDLSVLSIDLYKRVIVAMKARGVK

Table 2. Cont.

Motif No.	Motif Name	Sequence of Motifs
Motif 9	NPH3	SWKDSIIVLQTCENLLPLAEELKJVSRCIDSIASKACVD
Motif 10	NPH3	PGSPSLSSLVKVAKLVDGYLAEIAPDPNLKLSKFISLAE
Motif 11	N.A.	HALDLLAAADKYGVEQLKRLCEKALAEEDLSIENVLDVLQ
Motif 12	BTB	IKINDVPYEAFKAMLRFLYSGKLKEEPM
Motif 13	TAZ	PCSKFDTCQGLQLLIRHFATCKRRVPGGCJRCKRMWQILRLHSSICDQPDDCKVPLCRQFKZK
Motif 14	TAZ	NFKKIEETEGWKFLQHHPVLELEILQFMDEADJRKKRRRRRHKREQNLYLQLSEAMDCLEHI CREGCTSVGPHDKEP
Motif 15	NPR5/6	SHHHHEHDLSSADELEDKKIRRRRALDSDVELVLLLLMGEGLNLDEAIALHYAVEYCSRE VVKELLELG
Motif 16	NPR5/6	VVNPAGPRGKTPLHIAAERKEPDIIAVLLDKGADPNVRTLDGITPLDILRTLTR
Motif 17	ARM	HYEAVGVIGNLVHSSPNIKKEVLLAGALQPVIGLLSSCPESQREAALLLGQFAATSDCKIHI VQRGAVPPLIEMLQSPDAQLREMSAFALGRLAQDTHNQAGIAHCGGIPLKLLDSKNGSLQ HNAAFALYGLADNEDNVADLIKVGGVQKLQDGEFIVQPTRDCVAKTLKRLEEKIHGRILGHL LYLMRIGEKVIQ
Motif 18	NPH3	YAGETLYDVDTVQRILENFL
Motif 19	N.A.	ASLRRENRELKLELEKMRMRVADLEKEHVSMKQEIQK
Motif 20	NPH3	SEKKQRVILETIVSLLPKEKG

3.4. Phylogenetic Analysis

A phylogenetic analysis was performed using 57 StBTB proteins to analyze the evolutionary relationship within the BTB gene family in potato. Phylogenetic tree analysis showed that all the StBTBs were found to be broadly divided into three groups with Group I consisting of the NPR5/6 clade (StBTB11, StBTB19, StBTB31, StBTB33, StBTB35, and StBTB53). Group II consisted of six TAZ members (StBTB13, StBTB 18, StBTB26, StBTB27, StBTB38, and StBTB57), eight BTB proteins (StBTB9, StBTB20, StBTB22, StBTB25, StBTB30, StBTB36, StBTB48, and StBTB54), two ARM proteins (StBTB29 and StBTB45), and five MATH domain-containing proteins (StBTB1, StBTB3, StBTB23, StBTB46, and StBTB55). Group III consisted of six BACK proteins (StBTB5, StBTB39, StBTB40, 41, StBTB49, and StBTB56), one BTB protein (StBTB2), and 22 NPH3 proteins (StBTB4, StBTB6, StBTB7, StBTB8, StBTB10, StBTB12, StBTB14, StBTB15, StBTB16, StBTB17, StBTB21, StBTB24, StBTB28, StBTB32, StBTB34, StBTB37, StBTB42, StBTB43, StBTB44, StBTB47, StBTB50, and StBTB51) (Figure 4).

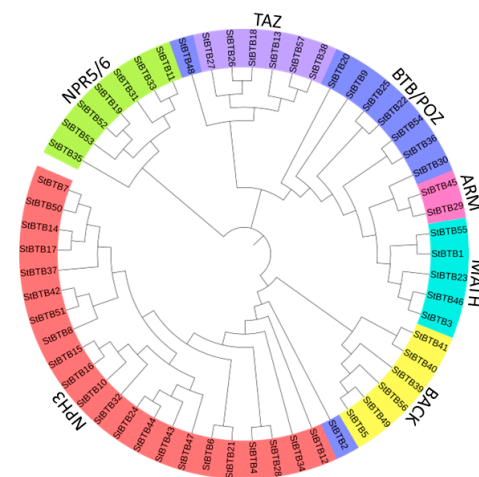


Figure 4. Phylogenetic tree showing the evolutionary relationship among StBTB proteins.

3.5. Tissue-Specific Gene Expression Analysis of *StBTBs*

The expression levels of *StBTBs* were analyzed in 16 different potato tissues (flower, leaf, petiole, shoot apex, stem, stolon, young tuber, mature tuber, root, stamen, water stressed leaf, tuber pith, tuber peel, whole in vitro plant, tuber sprout, and tuber cortex) (Supplementary File S1). All the *StBTBs* showed some level of expression in all the tissues, except *StBTB40*, which showed no expression in any tissues. *StBTB21*, *StBTB28*, *StBTB41*, and *StBTB57* also exhibited significantly low expression levels across all tissues. Overall, *StBTB26* showed the highest expression levels among all *StBTBs*, followed by *StBTB32*. The cumulative highest expression of all *StBTBs* was observed in the petiole followed by the water-stressed leaf, while the shoot apex and mature tuber exhibited the lowest expression levels. *StBTB32* showed the highest expression levels in the whole in vitro plant, followed by *StBTB26*, which showed the highest expression level in the petiole and water-stressed leaf of potato (Figure 5).

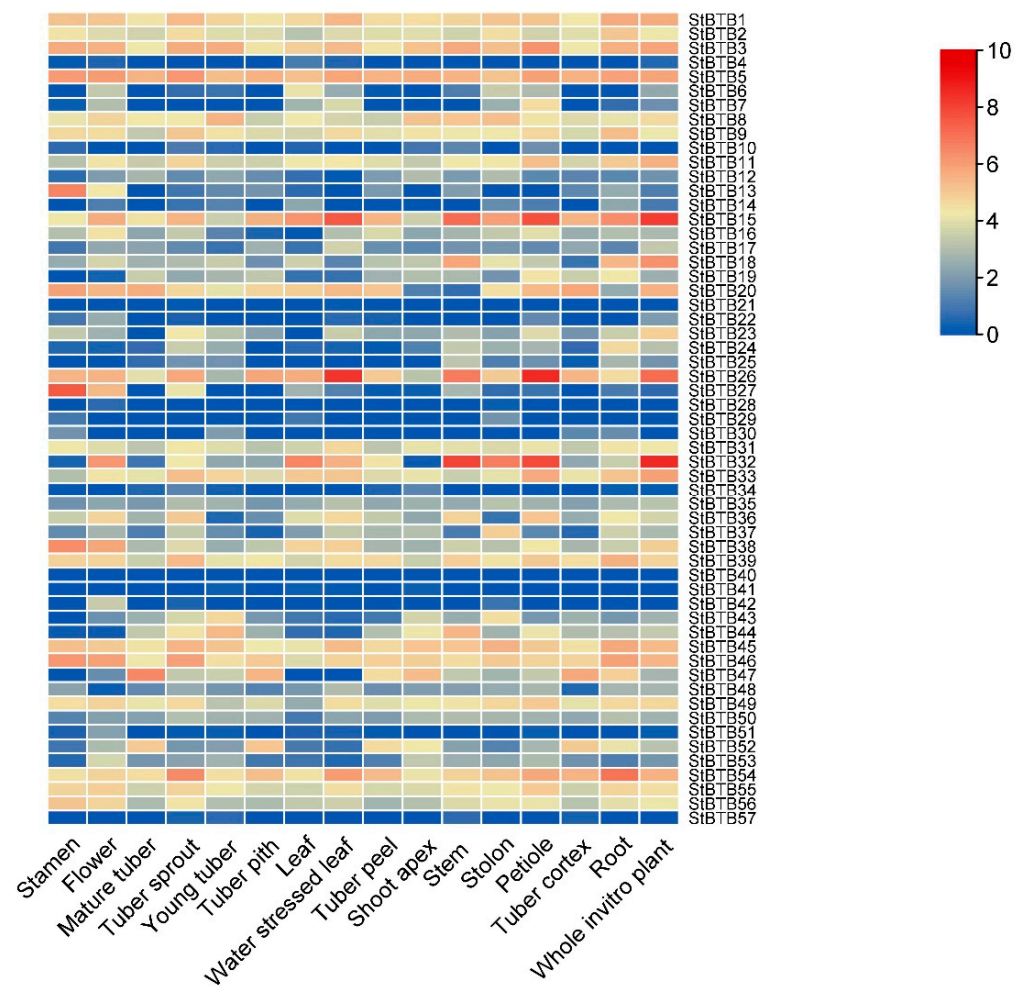


Figure 5. Heat map showing differential expression profiles of *StBTBs* in different potato tissues.

3.6. Expression Profile Analysis under Hormonal and Stress Treatments

The SRA (Sequence Read Archive) data of potato under hormonal treatments (BAP, ABA, IAA, and, GA3), abiotic stress (salt, mannitol, and heat), biotic stress (*P. infestans*), and SAR elicitors treatment (BABA and BTH) were used to analyze the differential expression levels of *StBTBs* (Supplementary File S1). *StBTB7* and *StBTB14* were found to be significantly downregulated under *P. infestans* infection with a log2fold change of -2.48 and -2.12 , respectively. Various *StBTBs*, namely *StBTB16*, *StBTB22*, *StBTB28*, and *StBTB29*, were observed to be upregulated under salt stress with log2fold changes of 2.41, 2.79, 2.23, and 6.41, respectively. Under drought stress due to mannitol treatment, *StBTB16*, *StBTB22*,

and *StBTB28* were upregulated with a log2fold change of 2.08, 3.31, and 2.09, respectively, while *StBTB23* was downregulated with a log2fold change of -2.45 . *StBTB17* and *StBTB19* were upregulated with log2fold changes of 2.15 and 2.23, and *StBTB53* was downregulated with a log2fold change of -3.97 . GA3 treatment led to *StBTB27* being upregulated with a log2fold change of 3.25 and *StBTB7* being downregulated with a log2fold change of -3.84 . *StBTB17* and *StBTB29* were downregulated with a log2fold change of -2.32 and -5.20 , while *StBTB22* was upregulated with a log2fold change of 2.67 under BAP treatment. *StBTB7* and *StBTB47* were downregulated with a log2fold change of -4.21 and -7.18 , while *StBTB27* was upregulated with a log2fold change of 2.93 under ABA treatment. Six *StBTBs* were observed to be downregulated, while *StBTB27* was upregulated under BABA treatment. *StBTB6* and *StBTB30* were upregulated, while *StBTB10*, *StBTB13*, and *StBTB18* were downregulated under BTH treatment (Figure 6).

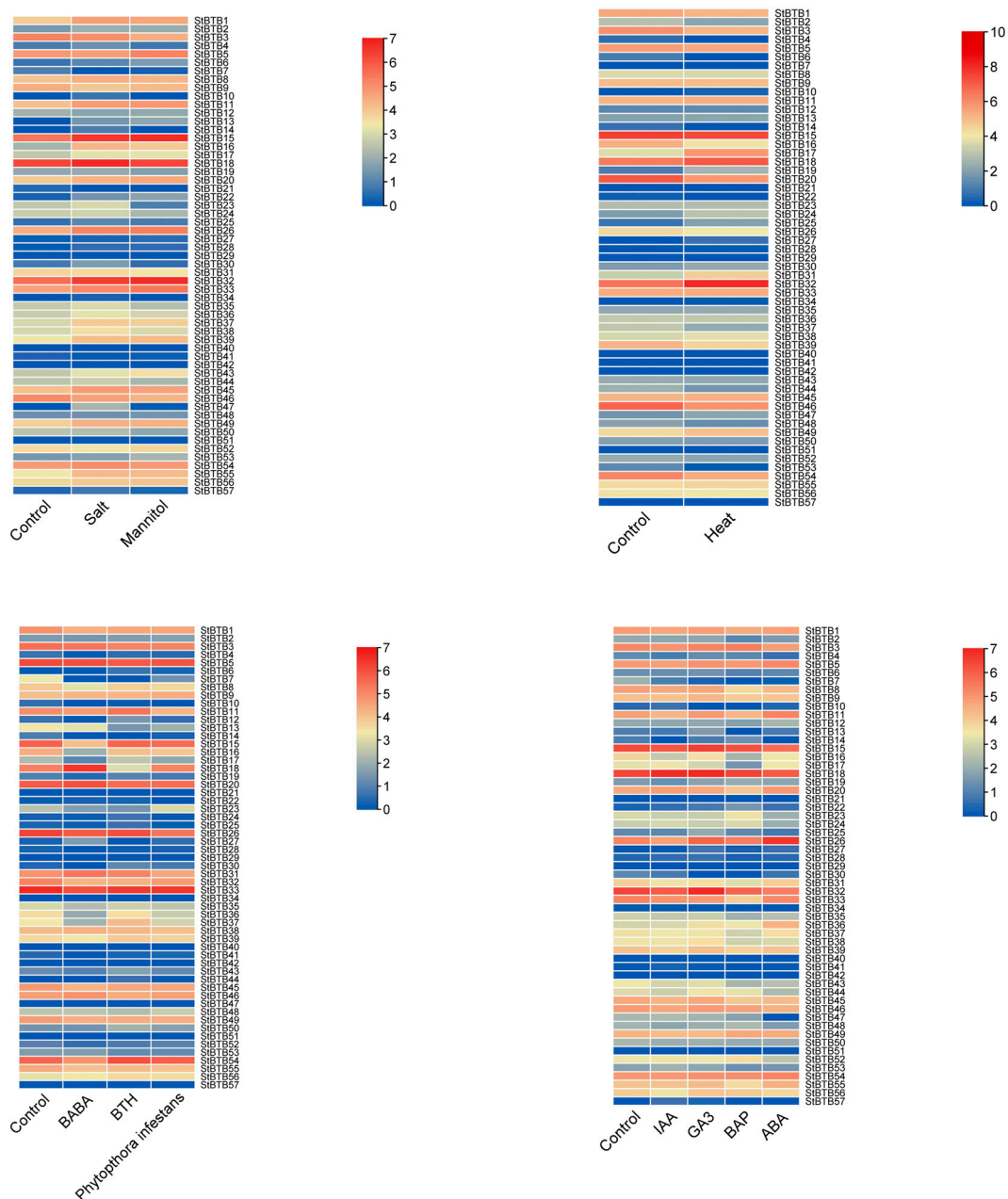


Figure 6. Heat maps showing differential expression of *StBTBs* under the treatment of salt, mannitol, heat, IAA, GA3, BAP, ABA, BABA, BTH, and *P. infestans*. (FPKM data for same have been provided in Supplementary File S1).

3.7. Protein–Protein Interaction and GO Analysis

StBTB48 was found to be the only BTB protein in potato interacting with various potato proteins such as M1CMR6 and M1BM03 (Ribosomal_L7Ae domain-containing protein); M1BJP4, M1D4J7, and M1CAV1 (Ribosomal_L18e/L15P domain-containing protein); M1BT69 (Ribosomal_L18_c domain-containing protein); M1CL91 (60S ribosomal protein L29); M1D4K6 and M1BIS3 (Ribosomal protein L19); Q3HVL2 (Ribosomal protein L27a-like protein); Q307Y8 (Ribosomal protein L11-like protein); M1BPE5 (40S ribosomal protein S24); M0ZQX8 (40S ribosomal protein S30); and some uncharacterized proteins including M1C6I6, M1B194, M1CKH6, M1CKD4, M0ZNS6, M1ATE7, and Q38HT5, all of which are most likely ribosomal proteins based on the domains present in these proteins (Figure 7).

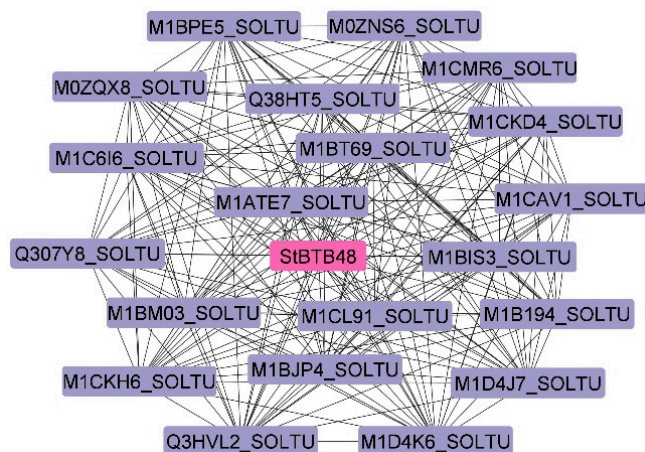


Figure 7. Protein–protein interaction network of StBTB proteins with other potato proteins with a high confidence score of 0.700 using String database.

Gene enrichment analysis revealed that the highest number of *StBTBs* (26) were involved in protein ubiquitination followed by the response to salicylic acid and hydrogen peroxide in terms of biological processes (Figure S1). In terms of molecular function, six *StBTBs* each were involved in metal ion binding and calmodulin binding. Sixteen *StBTBs* were found to be present in the nucleus. Thirty-three *StBTBs* were found to be involved in various metabolic processes such as nitrogen compound metabolic processes, cellular biosynthetic processes, protein metabolic processes, etc. Twenty-four *StBTBs* were involved in the response to a stimulus such as immune response, response to stress, response to abiotic and biotic stimuli, cellular response to chemical stimuli, response to endogenous stimuli, response to oxidative stress, etc. (Figure S2). The cellular component revealed that *StBTBs* were mostly associated with the cytoplasm, followed by the nucleus (Figure S3) (Table S3).

Pathway analysis revealed that 22 *StBTBs* were involved in peptidoglycan biosynthesis, while 16 *StBTBs* were involved in the hedgehog signaling pathway and 10 *StBTBs* were involved in alanine biosynthesis and cysteine degradation pathways.

3.8. microRNA Target Site Analysis

Various *StBTBs* were found to be targeted by several important miRNAs including 78 miRNA families targeting 53 out of 57 *StBTBs* (Table S4). Four *StBTBs* (*StBTB25*, *StBTB40*, *StBTB42*, and *StBTB51*) were not targeted by any miRNAs. *stu-miR5303* targeted 15 *StBTBs* (*StBTB1*, *StBTB3*, *StBTB5*, *StBTB7*, *StBTB10*, *StBTB12*, *StBTB21*, *StBTB32*, *StBTB33*, *StBTB33*, *StBTB34*, *StBTB35*, *StBTB38*, *StBTB43*, and *StBTB48*). The *stu-miR172* family was found to target ten *StBTBs* (*StBTB4*, *StBTB11*, *StBTB15*, *StBTB21*, *StBTB23*, *StBTB2831*, *StBTB32*, *StBTB33*, and *StBTB53*). *StBTB29* was targeted by the highest number of eight miRNA families. *Stu-miR1886* and *stu-miR1919* both targeted eight *StBTBs*, while *stu-miR7980* targeted seven *StBTBs*. *StBTB15* was found to be targeted by seven *stu-miRNA* families (Figure 8).

of BTBs present in various plants can clearly be seen. All the identified StBTB proteins had at least one BTB/POZ domain. Along with the BTB/POZ domain, many StBTB proteins were found to have several other domains such as NPH3, MATH, BACK, ARM, NPR5/6, and TAZ, all of which are involved in fundamental biological and molecular processes. The majority of the StBTB proteins were located in the nucleus, while a few were also located in the cytoplasm and chloroplast. *StBTB2* encoded a protein with the highest number of amino acid residues (865) and the highest molecular weight (94.892 kDa). The genes were unevenly distributed across all 12 chromosomes of potato, with chromosome 2 having the highest number of seven genes, and chromosomes 3, 4, 11, and 12 having only two genes each. Nine *StBTB* gene pairs were found to be duplicated within the potato genome, out of which two were tandemly duplicated, while the other seven were segmentally duplicated. All the duplicated genes were found to undergo purifying selection. Gene structure analysis revealed no significant pattern of intron–exon organization. The highest number of introns (18) was found in *StBTB48*, while the lowest number of introns (1) was found in *StBTB9*, *StBTB19*, *StBTB52*, and *StBTB53*. The longest intron was found in *StBTB31* with a length of 8871 bp. Conserved motif analysis revealed the presence of various motifs within StBTB proteins. BTB motifs were found in all the StBTB proteins. In addition to BTB, 22 StBTB proteins were observed to also contain NPH3 motifs, which suggests the role of these proteins in blue light-mediated phototropic responses [41]. The NPR5/6 motif was also found in seven StBTB proteins, indicating their role in leaf formation [42]. Six StBTB proteins constituted BACK motifs, which implies their role in plant ubiquitin degradation. The MATH domain, which is involved in the plant response to abiotic stress [43], was found in five StBTB proteins. The MATH domain-containing proteins within the BTB superfamily serve as substrate-specific adaptors for CULLIN (CUL3)-based ubiquitin E3 ligases, facilitating the targeting of proteins for ubiquitination [44]. Ubiquitin plays a significant role in various aspects such as cell cycle regulation, photomorphogenesis, self-incompatibility, circadian rhythms, flower development, hormonal balance, ecological adaptation, regulation of cell death, and disease resistance across all eukaryotes [45–48]. Five StBTB proteins (*StBTB13*, *StBTB18*, *StBTB26*, *StBTB27*, and *StBTB38*) consisted of the TAZ domain along with the BTB domain, which, in addition to playing a detrimental function in the ABA response, is a key player in a complex signaling network that senses and responds to hormones, stressors, and nutrients [19]. Two StBTB proteins consisted of the ARM domain, which along with the BTB/POZ domain has been shown to affect the stress tolerance of plants, seedling growth, and ABA-regulated gene expression in *Arabidopsis* [49]. Phylogenetic tree analysis showed that StBTB proteins containing the same domains were present within the same clade. Tissue-specific gene expression levels of all *StBTBs* were studied using the RNA-seq data of 16 different tissues of potato, namely flower, leaf, petiole, shoot apex, stem, stolon, young tuber, mature tuber, root, stamen, water stressed leaf, tuber pith, tuber peel, whole in vitro plant, tuber sprout, and tuber cortex. It was observed that *StBTB40*, a BTB/POZ-containing G-protein, did not show any level of expression in any of the aforementioned tissues. Except for this, all *StBTBs* showed expression in different potato tissues. This is in accordance with other studies that showed the involvement of BTBs in growth and development [16,39,50–53]. The BTB domain's significant contribution to plant growth and development is primarily due to its capability to interact with other functional domains, facilitated by the extension regions located at its N- and C-terminals [52]. Another investigation revealed that the BT2 gene enhanced telomerase expression in leaves [54]. *StBTB26* (BTB and TAZ domain protein), which is a stress-responsive protein, was observed to show the highest levels of expression across all the tissues. *StBTB32* (phototropic-responsive NPH3 family protein), which is involved in cellular protein modification processes, also showed the highest expression levels in the whole in vitro plant. Expression profile analysis revealed the role of various *StBTBs* in biotic and abiotic stress tolerance. Upon analyzing the SRA data, it was observed that *P. infestans* infection caused significant downregulation of *StBTB7* and *StBTB14*, both of which contained the NPH3 domain alongside the BTB domain. These

results are similar to the downregulation of a BTB domain-containing gene *CaBPM4* in response to *Phytophthora capsica* infection in pepper plants [55]. Overexpressed *GmBTB/POZ* also led to increased *Phytophthora sojae* resistance in soybean [56]. Transcriptome data of potato under salt stress showed significant upregulation in the expression of *StBTB16*, *StBTB22*, *StBTB28*, and *StBTB29*. *StBTB16*, *StBTB22*, and *StBTB28* were upregulated in response to drought stress in potato plants caused by mannitol treatment. BTB domain-containing genes have been studied and shown to be involved in both salt and drought stress. *AtSIBP1*, an Arabidopsis BTB protein, was observed to positively regulate the salt stress response in Arabidopsis [19]. In the case of drought stress, *MdBT2* is a negative regulator and causes drought sensitivity in apple [57]. On the other hand, *IbBT4*, a sweet potato BTB gene, confers drought tolerance when overexpressed in Arabidopsis [16]. When silenced, *CaBPM4* leads to improved tolerance under drought and salt stress exposure in pepper [55]. *StBTB7* (NPH3) was significantly downregulated, while *StBTB27* (TAZ) was significantly upregulated in response to both GA3 and ABA. Both these genes might prove to have a substantial role in hormone signaling and hence stress tolerance mechanisms. BT2, a BTB protein, has been shown to suppress ABA signaling in Arabidopsis [17]. It was reported that *GMPOZ*, a nuclear localized BTB/POZ domain protein, functioned as a repressor and activator of ABA- and GA-regulated genes in barley [58]. It was observed that BTB-MATH proteins have the capability to engage with homeodomain-leucine zipper transcription factors like ATHB6, thereby modulating phytohormone ABA responses and responses to abiotic stresses [44]. Studies showed that GA inhibited and induced *SIBTB12* and *SIBTB18*, respectively, in tomato plants [39]. It has been suggested that BT2 holds a central role within a complex signaling network that detects, integrates, and reacts to numerous, occasionally conflicting, signals. The hypothesis suggests its involvement in the formation of multiprotein complexes. Should the complex necessitate CULLIN3 or a comparable protein, it could potentially act as a ubiquitin ligase, marking specific proteins for degradation [17]. Several *StBTBs* were also found to be involved in the response to hydrogen peroxide, which might also explain their role in abiotic stress tolerance as *MdBT2*-overexpressed plants exhibited increased accumulation of H₂O₂, consequently leading to decreased drought stress tolerance [57]. Protein–protein interaction studies revealed no interaction among the BTB proteins of potato. However, *StBTB48* was observed to be interacting with 20 non-BTB proteins of potato. Interestingly, *StBTB48* does not contain any interacting domain other than BTB/POZ. All of the 20 interacting proteins were ribosomal proteins, which suggests the potential involvement of *StBTBs* in translation regulation, cellular signaling, and cellular stress response.

All *StBTBs* except *StBTB25*, *StBTB40*, *StBTB42*, and *StBTB51* were targeted by several miRNAs. Fifteen *StBTBs* were targeted by *stu-miR5303*, which potentially targets metabolic enzymes and proteins responsive to abiotic stress [59]. Ten *StBTBs* were targeted by *stu-miR172*, which plays a role in the tuberization process by regulating long-distance signals and targeting RAP1 mRNA and is involved in graft transmissible movement through the conductive vascular tissues [60]. *StBTB29* was observed to be targeted by eight different *stu-miRNA* families, which play various roles in plant development [61]. *stu-miR156*, which was first discovered to respond to cold stress in potato seedlings, plays various vital roles in the tuberization process, abiotic stress tolerance and controlling leaf development, apical dominance, and floral transition and development [62]. *stu-miR156* targeted four *StBTBs* including *StBTB22*, *StBTB31*, *StBTB45*, and *StBTB57*. Based on these results, potential *StBTB* gene candidates can be selected for further investigations regarding the stress mechanisms, hormone signaling pathways, and growth and development processes in potato and other plants.

5. Conclusions

In this study, we identified and characterized 57 *StBTBs* in the genome of *S. tuberosum* for the first time. Domain and motif analysis of the *StBTB* proteins revealed interaction of the BTB domain with other domains, namely NPH3, NPR5/6, TAZ, MATH, BACK,

and ARM. The majority of *StBTBs* showed tissue-specific expression, indicating their involvement in plant growth and development. Through differential expression studies, we predicted the role of various *StBTBs* in abiotic and biotic stresses and hormone signaling. Protein–protein interaction studies showed interaction of StBTB48 with ribosomal proteins, suggesting its role in translational regulation. We found 53 *StBTBs* were targeted by several miRNAs, indicating the role of miRNAs in regulating the expression of BTB domain-containing proteins. Our research introduces the initial comprehensive framework regarding the potato BTB domain-containing protein gene family, offering a foundational platform for subsequent in-depth investigations into the biological roles of the BTB domain in potato growth, development, hormone signaling, and responses to both abiotic and biotic stresses.

Supplementary Materials: The following supporting information can be downloaded at: <https://www.mdpi.com/article/10.3390/agriculture14050771/s1>, Table S1: Physicochemical properties of StBTB proteins; Table S2: Secondary structure composition of StBTB proteins; Table S3: GO IDs and names of *StBTBs*; Table S4: miRNAs targeting *StBTBs* and their mode of inhibition; Figure S1: Pie chart depicting biological process sequence distribution of *StBTBs*; Figure S2: Pie chart depicting molecular function sequence distribution of *StBTBs*; Figure S3: Pie chart depicting cellular component sequence distribution of *StBTBs*; Supplementary File S1: FPKM values for differential expression analysis. Sheet 1 shows data related to various stresses and sheet 2 for various developmental stages.

Author Contributions: A.: Data curation, formal analysis, methodology, roles/writing—original draft. A.K.: Software, validation. H.C.: Investigation, validation. S.K.U.: Data curation, writing—review and editing, supervision. K.S.: Conceptualization, funding acquisition, project administration, writing—review and editing. All authors have read and agreed to the published version of the manuscript.

Funding: The research was funded by Department of Biotechnology (DBT), India.

Data Availability Statement: The original contributions presented in the study are included in the Supplementary Materials, further inquiries can be directed to the corresponding author.

Conflicts of Interest: The authors declare no conflicts of interest.

References

- Bardwell, V.J.; Treisman, R. The POZ domain: A conserved protein–protein interaction motif. *Genes Dev.* **1994**, *8*, 1664–1677. [[CrossRef](#)] [[PubMed](#)]
- Zollman, S.; Godt, D.; Privé, G.G.; Couderc, J.L.; Laski, F.A. The BTB domain, found primarily in zinc finger proteins, defines an evolutionarily conserved family that includes several developmentally regulated genes in *Drosophila*. *Proc. Natl. Acad. Sci. USA* **1994**, *91*, 10717–10721. [[CrossRef](#)]
- Perez-Torrado, R.; Yamada, D.; Defosse, P.A. Born to bind: The BTB protein–protein interaction domain. *Bioessays* **2006**, *28*, 1194–1202. [[CrossRef](#)] [[PubMed](#)]
- Stogios, P.J.; Downs, G.S.; Jauhal, J.J.; Nandra, S.K.; Privé, G.G. Sequence and structural analysis of BTB domain proteins. *Genome Biol.* **2005**, *6*, R82. [[CrossRef](#)] [[PubMed](#)]
- Ahmad, K.F.; Engel, C.K.; Privé, G.G. Crystal structure of the BTB domain from PLZF. *Proc. Natl. Acad. Sci. USA* **1998**, *95*, 12123–12128. [[CrossRef](#)] [[PubMed](#)]
- Bonchuk, A.; Balagurov, K.; Georgiev, P. BTB domains: A structural view of evolution, multimerization, and protein–protein interactions. *Bioessays* **2023**, *45*, 2200179. [[CrossRef](#)] [[PubMed](#)]
- Nguyen, H.C.; Wang, W.; Xiong, Y. Cullin-RING E3 ubiquitin ligases: Bridges to destruction. *Macromol. Protein Complexes Struct. Funct.* **2017**, *83*, 323–347.
- Chaharbakhshi, E.; Jemc, J.C. Broad-complex, tramtrack, and bric-à-brac (BTB) proteins: Critical regulators of development. *Genesis* **2016**, *54*, 505–518. [[CrossRef](#)] [[PubMed](#)]
- Shalmani, A.; Ullah, U.; Muhammad, I.; Zhang, D.; Sharif, R.; Jia, P.; Saleem, N.; Gul, N.; Rakhmanova, A.; Tahir, M.M.; et al. The TAZ domain-containing proteins play important role in the heavy metals stress biology in plants. *Environ. Res.* **2021**, *197*, 111030. [[CrossRef](#)] [[PubMed](#)]
- Araus, V.; Vidal, E.A.; Puelma, T.; Alamos, S.; Mieulet, D.; Guiderdoni, E.; Gutiérrez, R.A. Members of BTB gene family of scaffold proteins suppress nitrate uptake and nitrogen use efficiency. *Plant Physiol.* **2016**, *171*, 1523–1532.
- Ahmad, K.F.; Melnick, A.; Lax, S.; Bouchard, D.; Liu, J.; Kiang, C.L.; Mayer, S.; Takahashi, S.; Licht, J.D.; Privé, G.G. Mechanism of SMRT corepressor recruitment by the BCL6 BTB domain. *Mol. Cell* **2003**, *12*, 1551–1564. [[CrossRef](#)] [[PubMed](#)]
- Siggs, O.; Beutler, B. The BTB-ZF transcription factors. *Cell Cycle* **2012**, *11*, 3358–3369. [[CrossRef](#)] [[PubMed](#)]

13. Ito, H.; Sato, K.; Yamamoto, D. Sex-switching of the *Drosophila* brain by two antagonistic chromatin factors. *Fly* **2013**, *7*, 87–91. [[CrossRef](#)] [[PubMed](#)]
14. Lim, J.H. Zinc finger and BTB domain-containing protein 3 is essential for the growth of cancer cells. *BMB Rep.* **2014**, *47*, 405. [[CrossRef](#)] [[PubMed](#)]
15. Geyer, R.; Wee, S.; Anderson, S.; Yates, J.; Wolf, D.A. BTB/POZ domain proteins are putative substrate adaptors for cullin 3 ubiquitin ligases. *Mol. Cell* **2003**, *12*, 783–790. [[CrossRef](#)] [[PubMed](#)]
16. Robert, H.S.; Quint, A.; Brand, D.; Vivian-Smith, A.; Offringa, R. BTB and TAZ domain scaffold proteins perform a crucial function in Arabidopsis development. *Plant J.* **2009**, *58*, 109–121. [[CrossRef](#)] [[PubMed](#)]
17. Mandadi, K.K.; Misra, A.; Ren, S.; McKnight, T.D. BT2, a BTB protein, mediates multiple responses to nutrients, stresses, and hormones in Arabidopsis. *Plant Physiol.* **2009**, *150*, 1930–1939. [[CrossRef](#)]
18. Zhou, Y.; Zhai, H.; He, S.; Zhu, H.; Gao, S.; Xing, S.; Wei, Z.; Zhao, N.; Liu, Q. The sweetpotato BTB-TAZ protein gene, IbBT4, enhances drought tolerance in transgenic Arabidopsis. *Front. Plant Sci.* **2020**, *11*, 877. [[CrossRef](#)] [[PubMed](#)]
19. Wan, X.; Peng, L.; Xiong, J.; Li, X.; Wang, J.; Li, X.; Yang, Y. AtSIBP1, a novel BTB domain-containing protein, positively regulates salt signaling in Arabidopsis thaliana. *Plants* **2019**, *8*, 573. [[CrossRef](#)]
20. Cao, H.; Li, X.; Dong, X. Generation of broad-spectrum disease resistance by overexpression of an essential regulatory gene in systemic acquired resistance. *Proc. Natl. Acad. Sci. USA* **1998**, *95*, 6531–6536. [[CrossRef](#)]
21. Zhao, M.; Ge, Y.; Xu, Z.; Ouyang, X.; Jia, Y.; Liu, J.; Zhang, M.; An, Y. A BTB/POZ domain-containing protein negatively regulates plant immunity in *Nicotiana benthamiana*. *Biochem. Biophys. Res. Commun.* **2022**, *600*, 54–59. [[CrossRef](#)]
22. Finn, R.D.; Clements, J.; Eddy, S.R. HMMER web server: Interactive sequence similarity searching. *Nucleic Acids Res.* **2011**, *39*, W29–W37. [[CrossRef](#)]
23. Lu, S.; Wang, J.; Chitsaz, F.; Derbyshire, M.K.; Geer, R.C.; Gonzales, N.R.; Gwadz, M.; Hurwitz, D.I.; Marchler, G.H.; Song, J.S.; et al. CDD/SPARCLE: The conserved domain database in 2020. *Nucleic Acids Res.* **2020**, *48*, D265–D268. [[CrossRef](#)]
24. Paysan-Lafosse, T.; Blum, M.; Chuguransky, S.; Grego, T.; Pinto, B.L.; Salazar, G.A.; Bileschi, M.L.; Bork, P.; Bridge, A.; Colwell, L.; et al. InterPro in 2022. *Nucleic Acids Res.* **2023**, *51*, D418–D427. [[CrossRef](#)] [[PubMed](#)]
25. Letunic, I.; Khedkar, S.; Bork, P. SMART: Recent updates, new developments and status in 2020. *Nucleic Acids Res.* **2021**, *49*, D458–D460. [[CrossRef](#)]
26. Gasteiger, E.; Hoogland, C.; Gattiker, A.; Duvaud, S.E.; Wilkins, M.R.; Appel, R.D.; Bairoch, A. *Protein Identification and Analysis Tools on the ExPASy Server*; Humana Press: Totowa, NJ, USA, 2005; pp. 571–607.
27. Horton, P.; Park, K.J.; Obayashi, T.; Fujita, N.; Harada, H.; Adams-Collier, C.J.; Nakai, K. WoLF PSORT: Protein localization predictor. *Nucleic Acids Res.* **2007**, *35*, W585–W587. [[CrossRef](#)]
28. Geourjon, C.; Deleage, G. SOPMA: Significant improvements in protein secondary structure prediction by consensus prediction from multiple alignments. *Bioinformatics* **1995**, *11*, 681–684. [[CrossRef](#)] [[PubMed](#)]
29. Shumayla, S.S.; Kumar, R.; Mendu, V.; Singh, K.; Upadhyay, S.K. Genomic dissection and expression profiling revealed functional divergence in *Triticum aestivum* leucine rich repeat receptor like kinases (TaLRRKs). *Front. Plant Sci.* **2016**, *7*, 1374. [[CrossRef](#)]
30. Chen, C.; Chen, H.; Zhang, Y.; Thomas, H.R.; Frank, M.H.; He, Y.; Xia, R. TBtools: An integrative toolkit developed for interactive analyses of big biological data. *Mol. Plant* **2020**, *13*, 1194–1202. [[CrossRef](#)] [[PubMed](#)]
31. Hu, B.; Jin, J.; Guo, A.Y.; Zhang, H.; Luo, J.; Gao, G. GSDS 2.0: An upgraded gene feature visualization server. *Bioinformatics* **2015**, *31*, 1296–1297. [[CrossRef](#)]
32. Bailey, T.L.; Johnson, J.; Grant, C.E.; Noble, W.S. The MEME suite. *Nucleic Acids Res.* **2015**, *43*, W39–W49. [[CrossRef](#)] [[PubMed](#)]
33. Edgar, R.C. MUSCLE: Multiple sequence alignment with high accuracy and high throughput. *Nucleic Acids Res.* **2004**, *32*, 1792–1797. [[CrossRef](#)] [[PubMed](#)]
34. Kumar, S.; Stecher, G.; Li, M.; Nnyaz, C.; Tamura, K. MEGA X: Molecular evolutionary genetics analysis across computing platforms. *Mol. Biol. Evol.* **2018**, *35*, 1547. [[CrossRef](#)] [[PubMed](#)]
35. Letunic, I.; Bork, P. Interactive Tree Of Life (iTOL) v5: An online tool for phylogenetic tree display and annotation. *Nucleic Acids Res.* **2021**, *49*, W293–W296. [[CrossRef](#)] [[PubMed](#)]
36. Szklarczyk, D.; Kirsch, R.; Koutrouli, M.; Nastou, K.; Mehryary, F.; Hachilif, R.; Gable, A.L.; Fang, T.; Doncheva, N.T.; Pyysalo, S.; et al. The STRING database in 2023: Protein–protein association networks and functional enrichment analyses for any sequenced genome of interest. *Nucleic Acids Res.* **2023**, *51*, D638–D646. [[CrossRef](#)] [[PubMed](#)]
37. Shannon, P.; Markiel, A.; Ozier, O.; Baliga, N.S.; Wang, J.T.; Ramage, D.; Amin, N.; Schwikowski, B.; Ideker, T. Cytoscape: A software environment for integrated models of biomolecular interaction networks. *Genome Res.* **2003**, *13*, 2498–2504. [[CrossRef](#)] [[PubMed](#)]
38. Dai, X.; Zhao, P.X. psRNATarget: A plant small RNA target analysis server. *Nucleic Acids Res.* **2011**, *39*, W155–W159. [[CrossRef](#)] [[PubMed](#)]
39. Li, J.; Su, X.; Wang, Y.; Yang, W.; Pan, Y.; Su, C.; Zhang, X. Genome-wide identification and expression analysis of the BTB domain-containing protein gene family in tomato. *Genes Genom.* **2018**, *40*, 1–15. [[CrossRef](#)] [[PubMed](#)]
40. Goyal, N.; Bhuria, M.; Verma, D.; Garewal, N.; Singh, K. Genome-Wide Identification of BTB Domain-Containing Gene Family in Grapevine (*Vitis vinifera* L.). *Agriculture* **2023**, *13*, 252. [[CrossRef](#)]
41. Motchoulski, A.; Liscum, E. Arabidopsis NPH3: A NPH1 photoreceptor-interacting protein essential for phototropism. *Science* **1999**, *286*, 961–964. [[CrossRef](#)]

42. Jun, J.H.; Ha, C.M.; Fletcher, J.C. BLADE-ON-PETIOLE1 coordinates organ determinacy and axial polarity in Arabidopsis by directly activating ASYMMETRIC LEAVES2. *Plant Cell* **2010**, *22*, 62–76. [[CrossRef](#)] [[PubMed](#)]
43. Kushwaha, H.R.; Joshi, R.; Pareek, A.; Singla-Pareek, S.L. MATH-domain family shows response toward abiotic stress in Arabidopsis and rice. *Front. Plant Sci.* **2016**, *7*, 923. [[CrossRef](#)] [[PubMed](#)]
44. Weber, H.; Bernhardt, A.; Dieterle, M.; Hano, P.; Mutlu, A.; Estelle, M.; Genschik, P.; Hellmann, H. Arabidopsis AtCUL3a and AtCUL3b form complexes with members of the BTB/POZ-MATH protein family. *Plant Physiol.* **2005**, *137*, 83–93. [[CrossRef](#)] [[PubMed](#)]
45. Gingerich, D.J.; Hanada, K.; Shiu, S.H.; Vierstra, R.D. Large-scale, lineage-specific expansion of a bric-à-brac/tramtrack/broad complex ubiquitin-ligase gene family in rice. *Plant Cell* **2007**, *19*, 2329–2348. [[CrossRef](#)] [[PubMed](#)]
46. Zapata, J.M.; Martínez-García, V.; Lefebvre, S. Phylogeny of the TRAF/MATH domain. In *TNF Receptor Associated Factors (TRAFs)*; Springer: Berlin/Heidelberg, Germany, 2007; pp. 1–24.
47. Qi, P.; Yan, H.; PeiFen, D.; QingXuan, X.; Ying, R.; ChunLin, L. Construction of SSH library with different stages of seeds development in *Brassica napus* L. *Acta Agron. Sin.* **2009**, *35*, 1576–1583.
48. Zhao, L.; Huang, Y.; Hu, Y.; He, X.; Shen, W.; Liu, C.; Ruan, Y. Phylogenetic Analysis of Brassica rapa MATH-Domain Proteins. *Curr. Genom.* **2013**, *14*, 214–223. [[CrossRef](#)] [[PubMed](#)]
49. Kim, S.Y.; Choi, H.I.; Korea Kumho Petrochemical Co., Ltd. Nucleic Acid Molecule Encoding an Armadillo Repeat Protein, Aria and a Method Utilizing Aria to Generate Salt Tolerant Plants. U.S. Patent 7,049,482, 3 May 2006.
50. Juranić, M.; Srilunchang, K.O.; Krohn, N.G.; Leljok-Levanić, D.; Sprunck, S.; Dresselhaus, T. Germline-specific MATH-BTB substrate adaptor MAB1 regulates spindle length and nuclei identity in maize. *Plant Cell* **2012**, *24*, 4974–4991. [[CrossRef](#)] [[PubMed](#)]
51. Gingerich, D.J.; Gagne, J.M.; Salter, D.W.; Hellmann, H.; Estelle, M.; Ma, L.; Vierstra, R.D. Cullins 3a and 3b assemble with members of the broad complex/ tramtrack/ bric-à-brac (BTB) protein family to form essential ubiquitin-protein ligases (E3s) in Arabidopsis. *J. Biol. Chem.* **2005**, *280*, 18810–18821. [[CrossRef](#)] [[PubMed](#)]
52. Shalmani, A.; Huang, Y.B.; Chen, Y.B.; Muhammad, I.; Li, B.B.; Ullah, U.; Jing, X.Q.; Bhanbhro, N.; Liu, W.T.; Li, W.Q.; et al. The highly interactive BTB domain targeting other functional domains to diversify the function of BTB proteins in rice growth and development. *Int. J. Biol. Macromol.* **2021**, *192*, 1311–1324. [[CrossRef](#)] [[PubMed](#)]
53. Juranić, M.; Dresselhaus, T. Phylogenetic analysis of the expansion of the MATH-BTB gene family in the grasses. *Plant Signal Behav.* **2014**, *9*, e28242. [[CrossRef](#)]
54. Ren, S.; Mandadi, K.K.; Boedeker, A.L.; Rathore, K.S.; McKnight, T.D. Regulation of telomerase in Arabidopsis by BT2, an apparent target of TELOMERASE ACTIVATOR1. *Plant Cell* **2007**, *19*, 23–31. [[CrossRef](#)] [[PubMed](#)]
55. He, Y.M.; Liu, K.K.; Zhang, H.X.; Cheng, G.X.; Ali, M.; Ul Haq, S.; Wei, A.M.; Gong, Z.H. Contribution of *CaBPM4*, a BTB domain-containing gene, to the response of pepper to *Phytophthora capsici* infection and abiotic stresses. *Agronomy* **2019**, *9*, 417. [[CrossRef](#)]
56. Zhang, C.; Gao, H.; Li, R.; Han, D.; Wang, L.; Wu, J.; Xu, P.; Zhang, S. GmBTB/POZ, a novel BTB/POZ domain-containing nuclear protein, positively regulates the response of soybean to *Phytophthora sojae* infection. *Mol. Plant Pathol.* **2019**, *20*, 78–91. [[CrossRef](#)] [[PubMed](#)]
57. Ji, X.L.; Li, H.L.; Qiao, Z.W.; Zhang, J.C.; Sun, W.J.; Wang, C.K.; Yang, K.; You, C.X.; Hao, Y.J. The BTB-TAZ protein MdBT2 negatively regulates the drought stress response by interacting with the transcription factor MdNAC143 in apple. *Plant Sci.* **2020**, *301*, 110689. [[CrossRef](#)] [[PubMed](#)]
58. Woodger, F.J.; Jacobsen, J.V.; Gubler, F. GMPOZ, a BTB/POZ domain nuclear protein, is a regulator of hormone responsive gene expression in barley aleurone. *Plant Cell Physiol.* **2004**, *45*, 945–950. [[CrossRef](#)] [[PubMed](#)]
59. Gu, M.; Liu, W.; Meng, Q.; Zhang, W.; Chen, A.; Sun, S.; Xu, G. Identification of microRNAs in six solanaceous plants and their potential link with phosphate and mycorrhizal signaling. *J. Integr. Plant Biol.* **2014**, *56*, 1164–1178. [[CrossRef](#)] [[PubMed](#)]
60. Martin, A.; Adam, H.; Diaz-Mendoza, M.; Zurczak, M.; Gonzalez-Schain, N.D.; Suarez-Lopez, P. Graft-transmissible induction of potato tuberization by the microRNA miR172. *Development* **2009**, *136*, 2873–2881. [[CrossRef](#)]
61. Pei, L.L.; Zhang, L.L.; Liu, X.; Jiang, J. Role of microRNA miR171 in plant development. *PeerJ* **2023**, *11*, e15632. [[CrossRef](#)]
62. Zhang, F.; Yang, J.; Zhang, N.; Wu, J.; Si, H. Roles of microRNAs in abiotic stress response and characteristics regulation of plant. *Front. Plant Sci.* **2022**, *13*, 919243. [[CrossRef](#)]

Disclaimer/Publisher’s Note: The statements, opinions and data contained in all publications are solely those of the individual author(s) and contributor(s) and not of MDPI and/or the editor(s). MDPI and/or the editor(s) disclaim responsibility for any injury to people or property resulting from any ideas, methods, instructions or products referred to in the content.